Search for Lorentz violations through the sidereal effect at the NOνA experiment

Shashank Mishra[1,2] Saurabh Shukla[1,2,*] Lakhwinder Singh[1,†] and Venktesh Singh[1]

[1]*Department of Physics, Central University of South Bihar, Gaya 824236, India*
[2]*Department of Physics, Institute of Science, Banaras Hindu University, Varanasi 221005, India*

Long-baseline neutrino oscillation experiments offer a unique laboratory to test the fundamental Lorentz symmetry, which is at the heart of both the standard model of particle and general relativity theory. The sidereal modulation in neutrino events will act as the smoking-gun experimental signature of Lorentz and *CPT* violation. In this study, we investigate the impact of the sidereal effect on standard neutrino oscillation measurements within the context of the NuMI Off-Axis ν_e Appearance Experiment (NOνA) experiment. Additionally, we assess the sensitivity of the NOνA experiment to detect Lorentz-violating interactions, taking into account the sidereal effect. Furthermore, we highlight the potential of the NOνA experiment to set new constraints on anisotropic Lorentz-violating parameters.

I. INTRODUCTION

Lorentz symmetry is a key assumption in our present understanding of high-energy processes and ensures that all inertial observers perceive the physical phenomenon identically. This symmetry, however, raises the question of testability in ultrahigh-energy theories at the Planck-scale physics such as string theory [1,2], loop quantum gravity [3], and braneworld scenarios [4]. These theories unify the gravity and gauge fields of the Standard Model (SM) of particle physics by allowing small perturbation of Lorentz symmetry, so-called Lorentz invariance violation (LIV) [5]. The Standard Model extension (SME) serves as an effective theory of above-mentioned ultrahigh-energy theories. The SME incorporates a complete range of particles and interactions of SM, as well as all possible Lorentz violation operators; therefore, it provides a feasible framework for LIV searches in a variety of scenarios like gravity, charged leptons, photons, nucleons, and neutrinos [6–8].

The discovery of "finite neutrino masses and mixings" with various neutrino sources is the first evidence of the existence of physics beyond the SM [9–11]. Over the last two decades, there has been tremendous development in neutrino experiments, allowing us to enter the era of precision measurement and the exploration of physics

beyond the Standard Model. The neutrino sector, therefore, offers a novel venue to explore the LIV effect. LIV parameters are classified as isotropic and anisotropic. In experiments where both the neutrino source and detector are located on the Earth, the observed sidereal modulation in neutrino events provides the smoking-gun signature of a nonzero anisotropic LIV parameters. Several neutrino experiments have performed the analysis to study the anisotropic LIV parameters including Liquid Scintillator Neutrino Detector (LSND) [12], Main Injector Neutrino Oscillation Search-Near Detector (MINOS-ND) [13,14], Mini Booster Neutrino Experiment (MiniBooNE) [15], IceCube [16], Double Chooz Reactor Neutrino Experiment (Double Chooz) [17], Tokai to Kamioka (T2K) [18], Daya Bay Reactor Neutrino Experiment (DayaBay) [19], etc. Previous experimental searches for LIV using the sidereal effect have primarily concentrated on short-baseline neutrino oscillation experiments. In long-baseline experiments, using MINOS-FD [20] and Super-K [21], an analysis was conducted on the directional and isotropic components of LIV, respectively.

The aim of this work is to expand and improve the sensitivity of LIV parameters in the nonisotropic time-dependence scenario. We investigate the sensitivity of the experiment towards non-isotropic LIV parameters in both appearance and disappearance channels by incorporating an effective Hamiltonian into the GLoBES software package. This allowed us to study the sidereal modulation of LIV parameters in the context of a long baseline neutrino experiment. This study mainly focuses on the FAR detector of NOνA experiment [22].

The article is structured as follows: The general formulation of the effective Hamiltonian is discussed in Sec. II.

---

*Corresponding author: saurabhshukla@cusb.ac.in
†Corresponding author: lakhwinder@cusb.ac.in

The effective Hamiltonian is also rearranged in simplified form to study the sidereal effect. Our approach to simulation, adopted experimental design, and standard oscillation parameters is outlined in Sec. III. In Sec. IV, we present the sensitivity of the NOνA experiment to explore LIV parameters with the marginalization over full parameter space of CP-violating phase (δ_{CP}) and θ_{23}. Additionally, we present upper limits for LIV parameters under sidereal analysis with realistic exposure for the NOνA experiment and compare them with existing upper limits of LIV parameters from the literature. The summary is given in Sec. V.

II. FORMALISM

In a lepton sector, the Lorentz-violating part of the SME Lagrangian can be divided into CPT-even and CPT-odd terms. The general form of Lorentz-violating part of the SME Lagrangian can be expressed as [6]

$$\mathcal{L}_{\mathrm{LIV}}^{CPT-\mathrm{even}} = -\frac{1}{2}(H_l)_{\mu\nu AB}\bar{l}_A\sigma^{\mu\nu}l_B + -\frac{1}{2}i(c_l)_{\mu\nu AB}\bar{l}_A\gamma^\mu\overleftrightarrow{D}^\nu l_B$$
$$+ -\frac{1}{2}i(d_l)_{\mu\nu AB}\bar{l}_A\gamma_5\gamma^\mu\overleftrightarrow{D}^\nu l_B, \quad (1)$$

where $(H_l)_{\mu\nu AB}$ are antisymmetric coupling coefficients with dimensions of mass. $(c_l)_{\mu\nu AB}$ and $(d_l)_{\mu\nu AB}$ are symmetric and antisymmetric Hermitian dimensionless CPT-even LIV coupling coefficients, respectively.

$$\mathcal{L}_{\mathrm{LIV}}^{CPT-\mathrm{odd}} = -(a_l)_{\mu AB}\bar{l}_A\gamma^\mu l_B - (b_l)_{\mu AB}\bar{l}_A\gamma_5\gamma^\mu l_B, \quad (2)$$

where $(a_l)_{\mu AB}$ and $(b_l)_{\mu AB}$ are Hermitian CPT-breaking LIV coupling coefficients with dimension of mass.

In the Hamiltonian picture, the effective Hamiltonian $(\mathcal{H}_{\mathrm{eff}})_{\alpha\beta}$ of neutrinos with small LIV and CPT-violating perturbation is generally written as [23]

$$(\mathcal{H}_{\mathrm{eff}})_{\alpha\beta} = (\mathcal{H}_o)_{\alpha\beta} + (\mathcal{H}_{LIV})_{\alpha\beta}, \quad (3)$$

where $(\mathcal{H}_o)_{\alpha\beta}$ is a conventional standard neutrino Hamiltonian that describes the Lorentz-invariant neutrino oscillation and $(\mathcal{H}_{\mathrm{LIV}})_{\alpha\beta}$ is a perturbative Hamiltonian including LIV contributions. The indices α and β represent the three neutrino flavors. In general, $(\mathcal{H}_{\mathrm{eff}})$ is a 6×6 matrix which can be represented as

$$(\mathcal{H}_{\mathrm{eff}}) = \begin{pmatrix} (\mathcal{H}_o)_{\nu\nu} & 0 \\ 0 & (\mathcal{H}_o)_{\bar{\nu}\bar{\nu}} \end{pmatrix} + \begin{pmatrix} (\mathcal{H}_{\mathrm{LIV}})_{\nu\nu} & (\mathcal{H}_{\mathrm{LIV}})_{\nu\bar{\nu}} \\ (\mathcal{H}_{\mathrm{LIV}})_{\bar{\nu}\nu} & (\mathcal{H}_{\mathrm{LIV}})_{\bar{\nu}\bar{\nu}} \end{pmatrix}, \quad (4)$$

where $(\mathcal{H}_o)_{\nu\nu}((\mathcal{H}_o)_{\bar{\nu}\bar{\nu}})$ is a standard neutrino (antineutrino) Hamiltonian term, which is responsible for standard neutrino (antineutrino) oscillations. Diagonal terms $(\mathcal{H}_{\mathrm{LIV}})_{\nu\nu}$

and $(\mathcal{H}_{\mathrm{LIV}})_{\bar{\nu}\bar{\nu}}$ contribute to neutrino-neutrino oscillation and antineutrino-antineutrino oscillation, respectively. Off-diagonal components, namely $(\mathcal{H}_{\mathrm{LIV}})_{\nu\bar{\nu}}$ and $(\mathcal{H}_{\mathrm{LIV}})_{\bar{\nu}\nu}$, govern neutrino-antineutrino oscillations and vice versa.

The standard neutrino(antineutrino) oscillation is parametrized by two mass-square differences Δm_{21}^2, Δm_{31}^2, three mixing angles θ_{12}, θ_{23}, θ_{13}, and a phase δ_{cp}. In this study, we solely conform to neutrino-neutrino oscillation, and corresponding Hamiltonian can be explicitly written as

$$(\mathcal{H}_o)_{\nu\nu} = \frac{1}{E}\left[U\begin{pmatrix} 0 & 0 & 0 \\ 0 & \Delta m_{21}^2 & 0 \\ 0 & 0 & \Delta m_{31}^2 \end{pmatrix}U^\dagger + V_{\mathrm{matter}}\right], \quad (5)$$

where the Pontecorvo–Maki–Nakagawa–Sakata (PMNS) matrix U is parameterized as Ref. [24] and V_{matter} is matter potential including the matter effect. In the minimal SME, the interactions and neutrino propagation are both governed by the following leading-order effective Hamiltonian [25]:

$$((\mathcal{H}_{eff})_{\nu\nu})_{\alpha\beta} = |\vec{p}|\delta_{\alpha\beta} + \frac{1}{|\vec{p}|}[(a_L)^\mu p_\mu - (c_L)^{\mu\nu}p_\mu p_\nu]_{\alpha\beta}, \quad (6)$$

where $(a_L)^\mu$ and $(c_L)^{\mu\nu}$ can be expressed as

$$(a_L)^\mu = \frac{1}{2}((a_l) + (b_l))^\mu, (c_L)^{\mu\nu} = \frac{1}{2}((c_l) + (d_l))^{\mu\nu}. \quad (7)$$

For simplicity we have dropped the suffix L in coefficients, which represents Left-handedness. $(a_L)^\mu$ and $(c_L)^{\mu\nu}$ are 3×3 complex matrices that represent LIV coefficients with mass dimensions 1 and 0, respectively. The 4-momentum $p_\mu = (|\vec{p}|, \vec{p})$ introduces the energy and momentum dependencies in the Hamiltonian. It implies that the mixing behavior of neutrino flavor depends on the direction of neutrino propagation which causes the rotational-symmetry violation. For the Earth-based experiment, where the source and detector are fixed on the Earth's surface, the rotation of the Earth around its axis generates sidereal variation in oscillation probabilities. This variation has a modulation with the Earth's sidereal rotation period (23 h 56 min solar hour). In order to compare the results from different experiments, it is convenient to adopt a common inertial frame. In the literature, measurements and sensitivities are conventionally expressed in terms of LIV coefficients defined in a Sun-centered celestial equatorial frame with coordinates (T, X, Y, Z).

The effective Hamiltonian with sidereal time dependencies in the Sun-centered celestial equatorial frame from Ref. [26] is restructured as follows:

$$(\mathcal{H}_{\text{LIV}})_{\alpha\beta} = (C)_{\alpha\beta} + R[a_{\alpha\beta}^X - 2E(c^{TX})_{\alpha\beta} + 2EN_z(c^{XZ})_{\alpha\beta}]\sin(\omega_\oplus T - \Phi_{\text{orientation}})$$
$$- R[a_{\alpha\beta}^Y - 2E(c^{TY})_{\alpha\beta} + 2EN_z(c^{YZ})_{\alpha\beta}]\cos(\omega_\oplus T - \Phi_{\text{orientation}})$$
$$+ R^2[E\frac{1}{2}((c^{XX})_{\alpha\beta} - (c^{YY})_{\alpha\beta})]\cos(2(\omega_\oplus T + \Phi_{\text{orientation}}))$$
$$+ R^2[E(c^{XY})_{\alpha\beta}]\sin(2(\omega_\oplus T - \Phi_{\text{orientation}})), \tag{8}$$

where T is the sidereal time, which describes the Earth's rotation with respect to a sidereal star in a Sun-centered frame. Amplitude $(C)_{\alpha\beta}$, $\Phi_{\text{orientation}}$, and R can be expressed in the directional factors N^X, N^Y, N^Z in the following manner:

$$\Phi_{\text{orientation}} = \tan^{-1}(N^Y/N^X),$$
$$R = \sqrt{N_X^2 + N_Y^2},$$
$$(C)_{\alpha\beta} = (a)_{\alpha\beta}^T - N^Z(a)_{\alpha\beta}^Z + E\left[-\frac{1}{2}(3 - N^Z N^Z)(c)_{\alpha\beta}^{TT}\right.$$
$$\left. + 2N^Z(c)_{\alpha\beta}^{TZ} + \frac{1}{2}(3 - N^Z N^Z)(c)_{\alpha\beta}^{ZZ}\right]. \tag{9}$$

The directional factors (N^X, N^Y, N^Z) are further expressed in terms of the angle between the beam and the vertically upward direction (θ) known as "zenith" angle; the angle between the beam and the south measured towards the east (ϕ) known as "bearing" angle; and the colatitude of the detector as (χ) [26]:

$$N^X = \cos\chi\sin\theta\cos\phi + \sin\chi\cos\theta,$$
$$N^Y = \sin\theta\sin\phi,$$
$$N^Z = -\sin\chi\sin\theta\cos\phi + \cos\chi\cos\theta. \tag{10}$$

The LIV coefficients $(a)_{\alpha\beta}^\mu$ are solely governed by the baseline, while coefficients $(c)_{\alpha\beta}^{\mu\nu}$ are subject to control from both the baseline length and the energy of the neutrinos. The parameters $(a)_{\alpha\beta}^T$, $(a)_{\alpha\beta}^Z$, $(c)_{\alpha\beta}^{TT}$, $(c)_{\alpha\beta}^{TZ}$, and $(c)_{\alpha\beta}^{ZZ}$ belong to $(C)_{\alpha\beta}$ and have no sidereal time dependency in the perturbation, while the parameters $(a)_{\alpha\beta}^X$, $(a)_{\alpha\beta}^Y$, $(c)_{\alpha\beta}^{TX}$, $(c)_{\alpha\beta}^{TY}$, $(c)_{\alpha\beta}^{XX}$, $(c)_{\alpha\beta}^{XY}$, $(c)_{\alpha\beta}^{XZ}$, $(c)_{\alpha\beta}^{YY}$, and $(c)_{\alpha\beta}^{YZ}$ are responsible for sidereal modulation of perturbed Hamiltonian terms. Nonisotropic LIV parameters suggest that the Universe has some preferred direction, i.e., the Universe is anisotropic in nature. However, there is no observed evidence supporting such anisotropy. Our objective of this study is to analyze the sensitivity of NOνA experiment, and set constraints on all 27 nondiagonal LIV parameters under the null hypothesis.

If the contribution of LIV perturbation in Eq. (3) is sufficiently small, the oscillation probabilities for both the appearance and disappearance channels can be expressed up to the leading order for the μe and $\mu\mu$ channels, similarly as presented in Refs. [27–34],

$$P_{\mu e}^{\text{LIV}} \simeq x^2 f^2 + 2xyfg\cos(\Delta + \delta_{CP}) + y^2 g^2 + 4r_A|h_{e\mu}^{\text{LIV}}|\left\{xf\left[fs_{23}^2\cos(\phi_{e\mu}^{\text{LIV}} + \delta_{CP}) + gc_{23}^2\cos(\Delta + \delta_{CP} + \phi_{e\mu}^{\text{LIV}})\right]\right.$$
$$+ yg\left[gc_{23}^2\cos\phi_{e\mu}^{\text{LIV}} + fs_{23}^2\cos(\Delta - \phi_{e\mu}^{\text{LIV}})\right]\right\} + 4r_A|h_{e\tau}^{\text{LIV}}|s_{23}c_{23}\left\{xf\left[f\cos(\phi_{e\tau}^{\text{LIV}} + \delta_{CP}) - g\cos(\Delta + \delta_{CP} + \phi_{e\tau}^{\text{LIV}})\right]\right.$$
$$- yg\left[g\cos\phi_{e\tau}^{\text{LIV}} - f\cos(\Delta - \phi_{e\tau}^{\text{LIV}})\right]\right\} + 4r_A^2 g^2 c_{23}^2|c_{23}|h_{e\mu}^{\text{LIV}}| - s_{23}|h_{e\tau}^{\text{LIV}}||^2 + 4r_A^2 f^2 s_{23}^2|s_{23}|h_{e\mu}^{\text{LIV}}| + c_{23}|h_{e\tau}^{\text{LIV}}||^2$$
$$+ 8r_A^2 fgs_{23}c_{23}\left\{c_{23}\cos\Delta\left[s_{23}(|h_{e\mu}^{\text{LIV}}|^2 - |h_{e\tau}^{\text{LIV}}|^2) + 2c_{23}|h_{e\mu}^{\text{LIV}}||h_{e\tau}^{\text{LIV}}|\cos(\phi_{e\mu}^{\text{LIV}} - \phi_{e\tau}^{\text{LIV}})\right]\right.$$
$$\left. - |h_{e\mu}^{\text{LIV}}||h_{e\tau}^{\text{LIV}}|\cos(\Delta - \phi_{e\mu}^{\text{LIV}} + \phi_{e\tau}^{\text{LIV}})\right\} + \mathcal{O}(s_{13}^2 a, s_{13}a^2, a^3), \tag{11}$$

$$P_{\mu\mu}^{\text{LIV}} \simeq 1 - \sin^2 2\theta_{23}\sin^2\Delta - |h_{\mu\tau}^{\text{LIV}}|\cos\phi_{\mu\tau}^{\text{LIV}}\sin 2\theta_{23}[(2r_A\Delta)\sin^2 2\theta_{23}\sin 2\Delta + 4\cos^2 2\theta_{23}r_A\sin^2\Delta]$$
$$+ (|h_{\mu\mu}^{\text{LIV}}| - |h_{\tau\tau}^{\text{LIV}}|)\sin^2 2\theta_{23}\cos 2\theta_{23}[(r_A\Delta)\sin 2\Delta - 2r_A\sin^2\Delta], \tag{12}$$

where

$$s_{ij} = \sin\theta_{ij}, \qquad c_{ij} = \cos\theta_{ij}, \qquad x = 2s_{13}s_{23}, \qquad y = 2rs_{12}c_{12}c_{23}, \qquad r = |\Delta m_{21}^2/\Delta m_{31}^2|, \qquad \Delta = \frac{\Delta m_{31}^2 L}{4E},$$

$$V_{CC} = \sqrt{2}G_F N_e, \qquad r_A = \frac{2E}{\Delta m_{31}^2}, \qquad f = \frac{\sin[\Delta(1 - r_A(V_{CC} + h_{ee}^{\text{LIV}}))]}{1 - r_A(V_{CC} + h_{ee}^{\text{LIV}})}, \qquad g = \frac{\sin[\Delta r_A(V_{CC} + h_{ee}^{\text{LIV}})]}{r_A(V_{CC} + h_{ee}^{\text{LIV}})}. \tag{13}$$

The antineutrino probability $P_{\bar\mu\bar e}^{\mathrm{LIV}}$ ($P_{\bar\mu\bar\mu}^{\mathrm{LIV}}$) can be obtained from Eq. (11) [Eq. (12)] by replacing $V_{CC} \to -V_{CC}$, $\delta_{CP} \to -\delta_{CP}$, and $a_{\alpha\beta} \to -a_{\alpha\beta}^*$. Similar expression for inverse hierarchy can be obtained by substituting $\Delta m_{31}^2 \to -\Delta m_{31}^2$, i.e., $\Delta \to -\Delta$ and $r_A \to -r_A$.

III. NUMERICAL PROCEDURE OF SIMULATION

NuMI Off-Axis ν_e Appearance Experiment (NOνA), a long baseline experiment at Fermilab, examines neutrino oscillations using a high-intensity and high-purity beam of either muon neutrinos or muon antineutrinos. The experiment utilizes two identical detectors: a far detector (FD) and a near detector (ND). The fiducial mass of FD is 14 kTon, and it is situated 810 KM away from the target and 14 mRad off axis [35]. As a fixed baseline experiment, NOνA can observe the sidereal variation in the neutrino event rate in FD arising due to the Earth's rotation. In order to study the oscillation probabilities and event rate for NOνA experiment, we adopted the GLoBES [36,37] software package with suitable modifications in *snu.c* plugin to include the sidereal effect. A exposure total of 2.5×10^{21} protons on target (POT) is utilized for the analysis of neutrinos, and an identical exposure is applied for antineutrinos. The POT is independent of sidereal time and remains constant throughout the time bin. For both the appearance and disappearance channels, the energy window is fixed from 1.0 to 5.0 GeV, with a peak value at 2.0 GeV.

Table I provides a summary of the standard oscillation parameters used in this work. Since NOνA is not sensitive for the mixing angles θ_{12} and θ_{13} [38] and these parameters are well measured by other neutrino oscillation experiments, hence their values are fixed in simulation. As the sidereal effect is time dependent, the flux variation with sidereal time may alter the event to local sidereal time (LST) spectra. Since there are no prior experimental data available on flux variation with LST, an average constant flux over the entire sidereal period is considered.

The latest data of NOνA experiment favor the normal neutrino mass hierarchy by 1.9σ [22]; therefore, the normal mass ordering is also fixed throughout the simulation. Details on the beam orientation and FD of NOνA experiment, which is employed for the simulation, are represented

TABLE I. The standard oscillation parameters are used in this work [39].

Parameter	True value	Test value
θ_{12}	33.48°	
θ_{13}	8.5°	
θ_{23}	45.0°	(41.0°, 52.0°)
δ_{cp}	195.0°	(0°, 360.0°)
$\triangle m_{21}^2$	7.55×10^{-5} eV²	
$\triangle m_{31}^2$	2.50×10^{-3} eV²	

TABLE II. NOνA FD orientation details used in the simulation [35].

Parameter	Value
χ colatitude	48.3793°
θ zenith angle	84.26°
ϕ bearing	204.616°

in Table II. The value of $\Phi_{\mathrm{orientation}}$ is fixed for the NOνA experiment using the colatitude, zenith, and bearing angle.

IV. RESULTS AND DISCUSSION

The standard neutrino oscillation probability spectrum without LIV parameters for appearance and disappearance channels with respect to energy and local sidereal time (LST) is depicted at the top and bottom of Fig. 1, respectively. All energies of neutrinos have a smooth
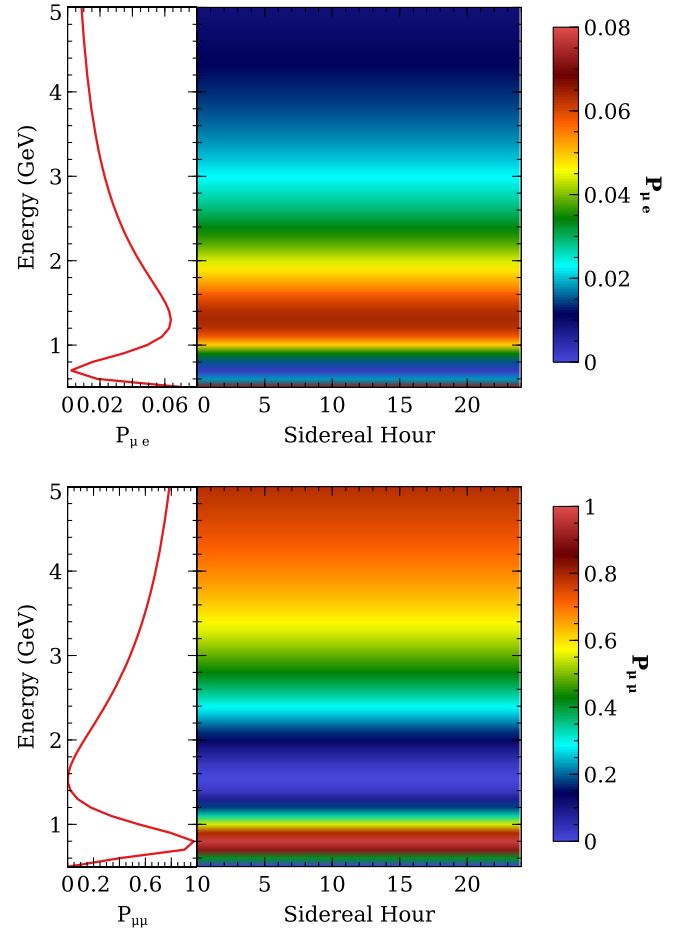

FIG. 1. The standard neutrino oscillation 1D probability spectrum in terms of energy, as well as the probability distribution in terms of local sidereal time (LST) and energy for the appearance channel (top) and disappearance channel (bottom) without taking LIV parameters into account. The oscillation parameters listed in Table I are adopted to calculate the probability distribution.

probability distribution throughout the whole sidereal time. However, there is a considerable distortion in the standard neutrino oscillation probability distribution when LIV parameters are taken into account. In order to analyze the impact of individual LIV parameters on the probability-LST distribution, all LIV parameters, excluding the one under consideration, are set to zero. The nonzero value of the mass dimension LIV parameter $(a)^\mu$ is set to 1×10^{-23} GeV, and a dimensionless parameter $(c)^{\mu\nu}$ is assigned the same order of value. The probability distribution difference between SM and LIV for the appearance and disappearance channels is shown in Figs. 2 and 3, respectively. The first, second, third, fourth, and fifth panels (from left to right) of Figs. 2 and 3 illustrate the distortion in the standard neutrino oscillation probability distribution, when $(a^X)_{\alpha\beta}$, $(c^{TX})_{\alpha\beta}$, $(c^{XX})_{\alpha\beta}$, $(c^{XZ})_{\alpha\beta}$, and $(c^{XY})_{\alpha\beta}$ parameters are set to nonzero value, respectively. The top, middle, and bottom panels represent $\alpha\beta = e\mu$, $e\tau$, and $\mu\tau$ coefficients, respectively.

As we move from left to right in the top panel of Figs. 2 and 3, the probability modulates as $\omega_\oplus$, $\omega_\oplus$, $2\omega_\oplus$, $\omega_\oplus$, and $2\omega_\oplus$. This nature is fairly evident for $e\mu$ and $e\tau$ coefficients in the appearance channel as well as $\mu\tau$ coefficients in the disappearance channel. Such modulations in the data serve as a smoking-gun signature for LIV.

One can notice that the amplitude of modulation due to CPT-conserving parameters $(c)^{TX}$, $(c)^{XZ}$, $(c)^{XX}$, and $(c)^{XY}$ is more significant than those of the CPT-violating parameters $(a)^X$ or $(a)^Y$ in the probability difference

distribution for both the appearance and disappearance channels. This increase in amplitude is attributed to the presence of neutrino energy in CPT-conserving terms. The strength of modulation in $(c)^{TX}_{e\mu}$ and $(c)^{XZ}_{e\mu}$ is stronger than other CPT-conserving parameters due to the orientation of the NOνA experiment. The LIV parameters associated with the $e\mu$ and $e\tau$ coefficients do not play a significant role in the disappearance channel. This is evident as they do not appear in the leading-order term of the disappearance channel probability.

Figures 8 and 9 as shown in the Appendix illustrate the nature of the contribution of Y-type components (a^Y, c^{TY}, c^{YY}, c^{YZ}). The phase shift between X-type (a^X, c^{TX}, c^{XX}, c^{XZ}) and Y-type (a^Y, c^{TY}, c^{YY}, c^{YZ}) components is 6 sidereal hour, and this shift can be understood with the structure of the Hamiltonian of the LIV perturbation as shown in Eq. (8), since X-type components appear with a sinusoidal term while Y-type components appear with a cosine term. In the null-hypothesis analysis for individual components, the constraints will be the same for X- and Y-type LIV parameters. Hence, the next sections exclusively focus on the discussion and graphical representation of parameters a^X, c^{TX}, c^{XX}, c^{XZ}, c^{XY}.

The primary objectives of all ongoing and prospective high-precision, long-baseline neutrino oscillation experiments are to determine the precise CP-violating phase (δ_{cp}) and the octant of θ_{23}, as well as to resolve the mass hierarchy. However, there are significant uncertainties in the current measurement of the θ_{23} and δ_{cp} phase. In the

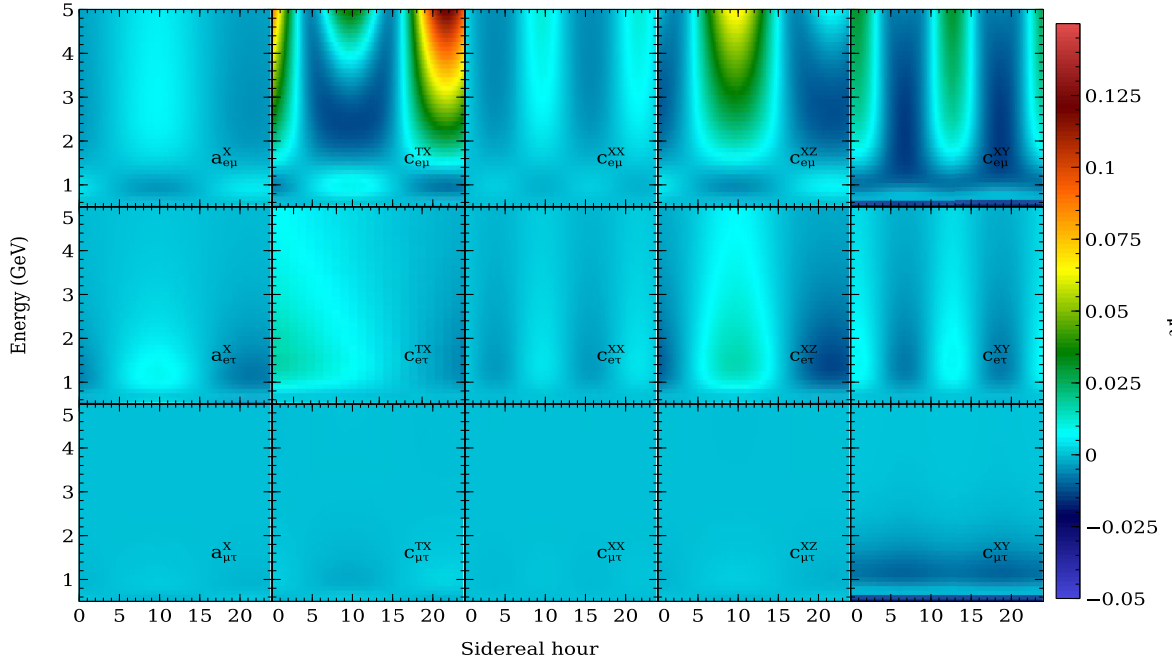
FIG. 2. The probability difference distribution for the appearance channel for X-type components ($a^X_{\alpha\beta}$, $c^{TX}_{\alpha\beta}$, $c^{XX}_{\alpha\beta}$, $c^{XZ}_{\alpha\beta}$, $c^{XY}_{\alpha\beta}$, with $\alpha\beta = e\mu$, $e\tau$, and $\mu\tau$). In each panel, one specific LIV parameter is set to 1×10^{-23}, while the others are set to 0.
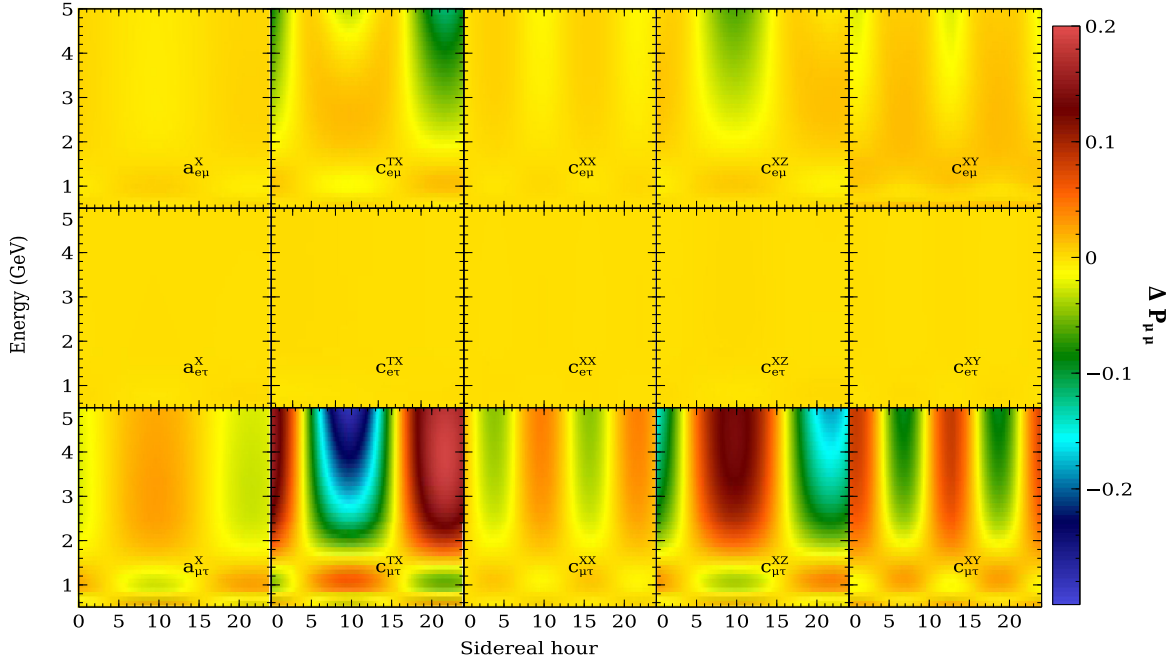
FIG. 3.   The probability difference distribution for the disappearance channel for X-type components ($a^X_{\alpha\beta}$, $c^{TX}_{\alpha\beta}$, $c^{XX}_{\alpha\beta}$, $c^{XZ}_{\alpha\beta}$, $c^{XY}_{\alpha\beta}$, with $\alpha\beta = e\mu$, $e\tau$, and $\mu\tau$). In each panel, one specific LIV parameter is set to 1×10^{-23}, while the others are set to 0.

case of long-baseline searches, standard oscillation parameters mix with the LIV parameter. The unknown standard oscillation parameters (δ_{CP}, θ_{23}) introduce a level of uncertainty that can potentially reduce the sensitivity of the experiment to detect the sidereal signal. We therefore investigate the correlations between the LIV parameters and conventional oscillation parameters θ_{23} and δ_{CP}.

In order to derive the sensitivity, we adopt the Poisson-likelihood chi-square statistics. The Poisson-likelihood chi-square function for NOνA experiment can be written as [40]

$$\chi^2_{\text{total}}(N_{\text{test}}, N_{\text{true}})$$
$$= \sum_{i,j,k} 2\left(N^{ijk}_{\text{test}} - N^{ijk}_{\text{true}} + N^{ijk}_{\text{true}} \times \ln\left[\frac{N^{ijk}_{\text{true}}}{N^{ijk}_{\text{test}}} \right] \right), \quad (14)$$

where "i" stands for LST bins, "j" for appearance and disappearance channels, and "k" for the beam's neutrino and antineutrino modes. "N_{true}" represents the total number of events in each sidereal bin for an energy window of 1 to 5 GeV in the SM case, while "N_{test}" represents the same quantity in the case of LIV. We adopt 24 sidereal bins, each spanning one sidereal hour, covering the entire duration of a sidereal day. The total 5% of systematic uncertainty is considered in the final analysis. Systematics is incorporated using the so-called pull method.

The strength of a LIV parameter depends on its phase; therefore, the sensitivity of an experiment to a particular LIV parameter is influenced by the phase of that parameter. As the phases of these parameters are unknown, we

perform the marginalization over the full parameter space of the LIV phase ($\phi_{\text{parameter}}$) along with the uncertainty range of δ_{CP} to investigate the correlation between LIV parameters and θ_{23}. Figure 4 illustrates the correlation between δ_{CP} and nondiagonal LIV parameters ($a^X_{\alpha\beta}$, $c^{TX}_{\alpha\beta}$, $c^{XX}_{\alpha\beta}$, $c^{XY}_{\alpha\beta}$, $c^{XZ}_{\alpha\beta}$ with $\alpha\beta = e\mu$, $e\tau$, and $\mu\tau$) at the 2σ, 2.5σ, and 3σ significance level. The contribution of LIV parameters corresponding to the $e\tau$ coefficient for the appearance channel in oscillation probability is suppressed by approximately a factor of 2, due to the $\sin(\theta_{23})\cos(\theta_{23})$ term. Therefore, the sensitivity of these parameters degrades as compared to the LIV parameters corresponding to $e\mu$ coefficient for the appearance channel. Figure 5 shows correlation between δ_{CP} phase and nondiagonal LIV parameters at 2σ, 2.5σ, and 3σ significance level with marginalizing over both $\phi_{\text{parameter}}$ and θ_{23}. To assess the sensitivity of NOνA to the nondiagonal LIV parameters and across the entire range of corresponding phase values, we marginalize over the θ_{23} and δ_{CP} phase. Figure 6 illustrates the allowed region of nondiagonal LIV parameters with respect to the entire range of corresponding $\phi_{\text{parameter}}$ at 2σ, 2.5σ, and 3σ significance levels. The nondiagonal LIV parameters associated with $\mu\tau$ occur with the δ_{CP} phase, whereas the parameters linked to $e\mu$ and $e\tau$ do not exhibit such dependency. The sensitivity of nondiagonal LIV parameters corresponding to the $\mu\tau$ disappearance channel is enhanced when the parameter is purely real compared to purely imaginary. On the contrary, the nondiagonal LIV parameters corresponding to $e\mu$ and $e\tau$ appearance channels exhibit a less-pronounced
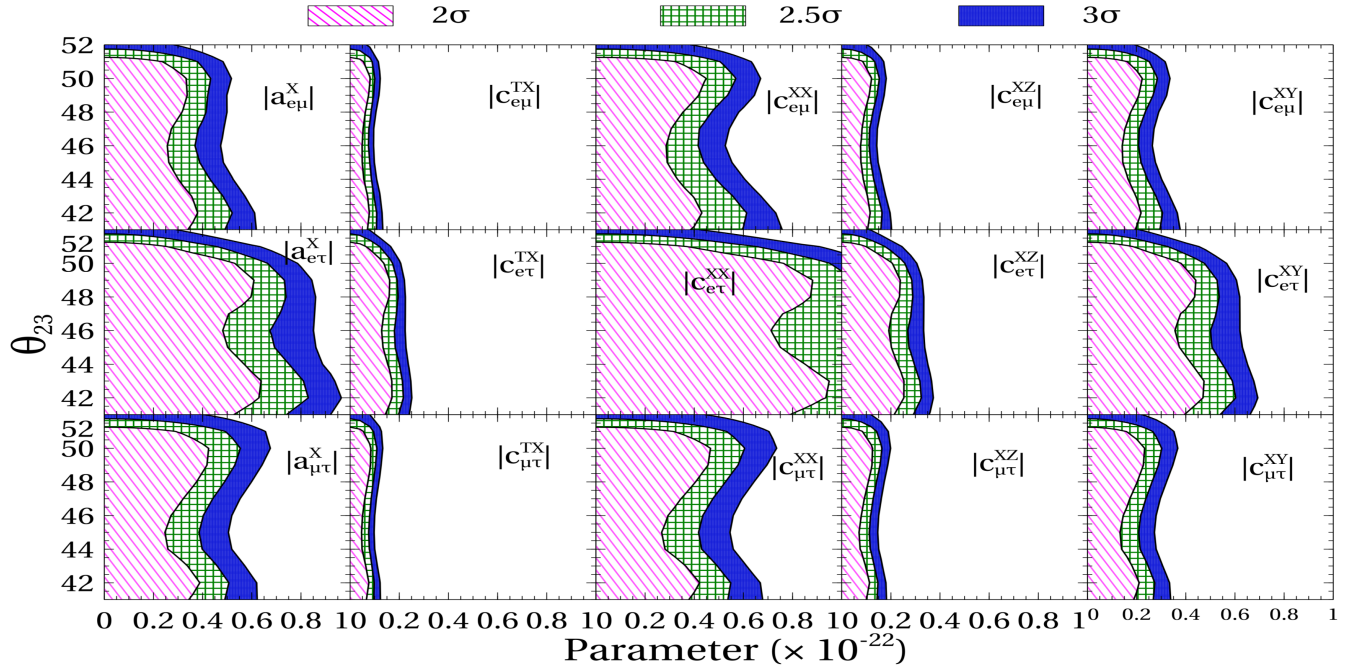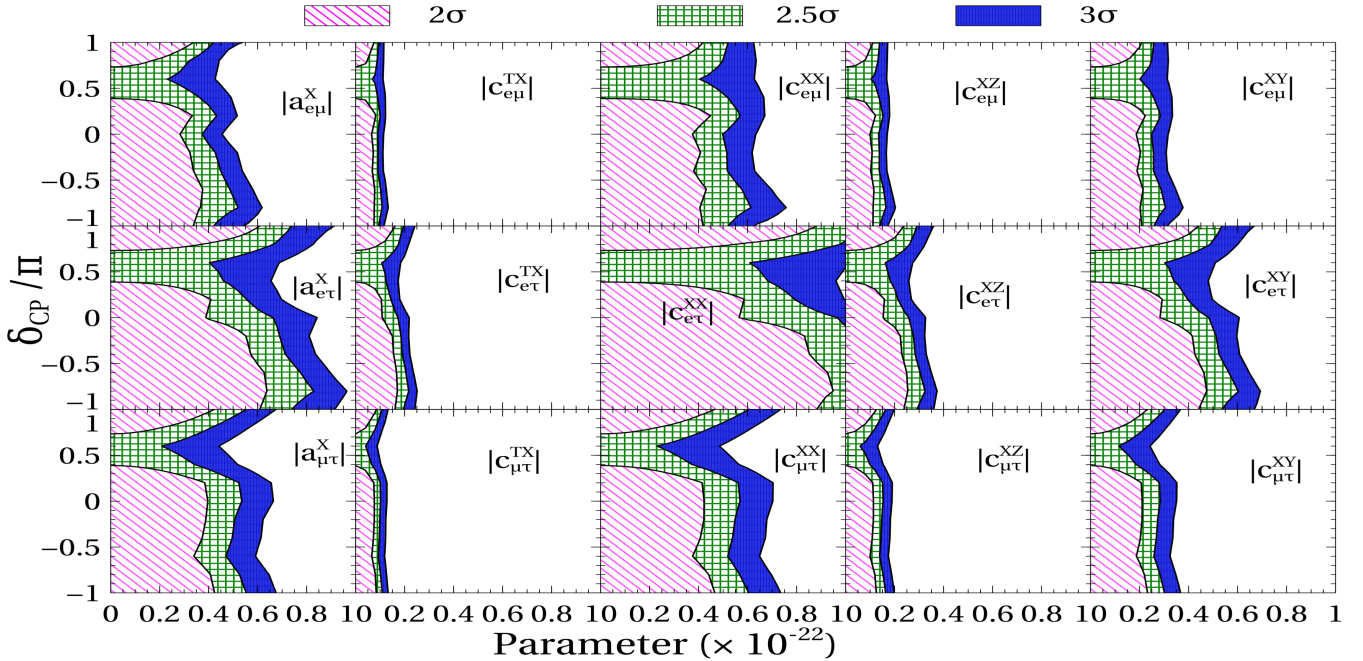
FIG. 4. Correlations between the nondiagonal parameters ($a_{\alpha\beta}^X$, $c_{\alpha\beta}^{TX}$, $c_{\alpha\beta}^{XX}$, $c_{\alpha\beta}^{XZ}$, $c_{\alpha\beta}^{XY}$ with $\alpha\beta = e\mu$, $e\tau$, and $\mu\tau$) and mixing angle θ_{23} at 2σ, 2.5σ, and 3σ confidence level (CL).

FIG. 5. Correlations between the nondiagonal parameters ($a_{\alpha\beta}^X$, $c_{\alpha\beta}^{TX}$, $c_{\alpha\beta}^{XX}$, $c_{\alpha\beta}^{XZ}$, $c_{\alpha\beta}^{XY}$ with $\alpha\beta = e\mu$, $e\tau$, and $\mu\tau$) and Dirac CP phase δ_{CP} at 2σ, 2.5σ, and 3σ CL.

manifestation of this characteristic due to the marginalization over the δ_{CP} phase.

Figure 7 illustrates the χ^2 sensitivity of the LIV parameters in both the appearance and disappearance channels, considering both neutrino and antineutrino modes. By adopting a one-parameter-at-a-time analysis, the upper limits at the 3σ level of all 27 LIV parameters are listed in Table III. We note that sidereal analysis with FAR detector provides more stringent constraints on the 3σ level for the CPT-violating coefficient $a_{e\mu}^X$ ($a_{e\mu}^Y$) in the null hypothesis. These constraints are now suppressed by three orders of magnitude compared to the previously reported
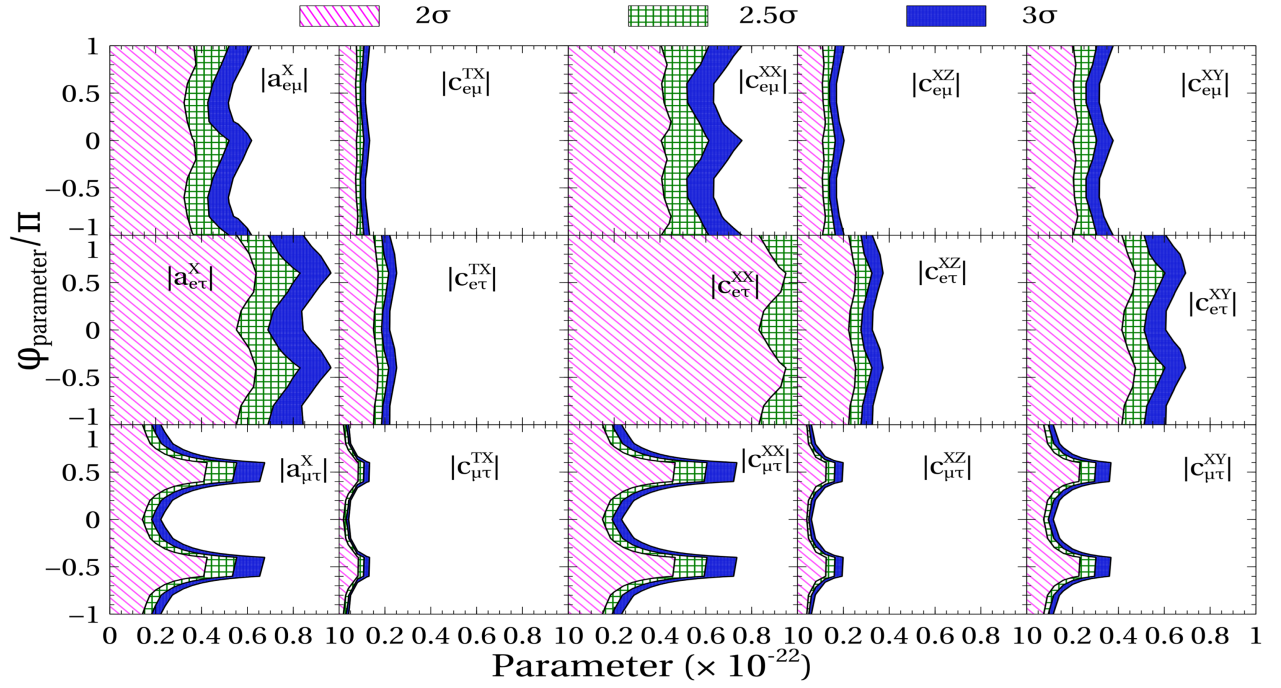
FIG. 6. Correlations between the nondiagonal parameters ($a_{\alpha\beta}^X$, $c_{\alpha\beta}^{TX}$, $c_{\alpha\beta}^{XX}$, $c_{\alpha\beta}^{XZ}$, $c_{\alpha\beta}^{XY}$ with $\alpha\beta = e\mu$, $e\tau$, and $\mu\tau$) and $\Phi_{\text{parameter}}$ at 2σ, 2.5σ, and 3σ CL.
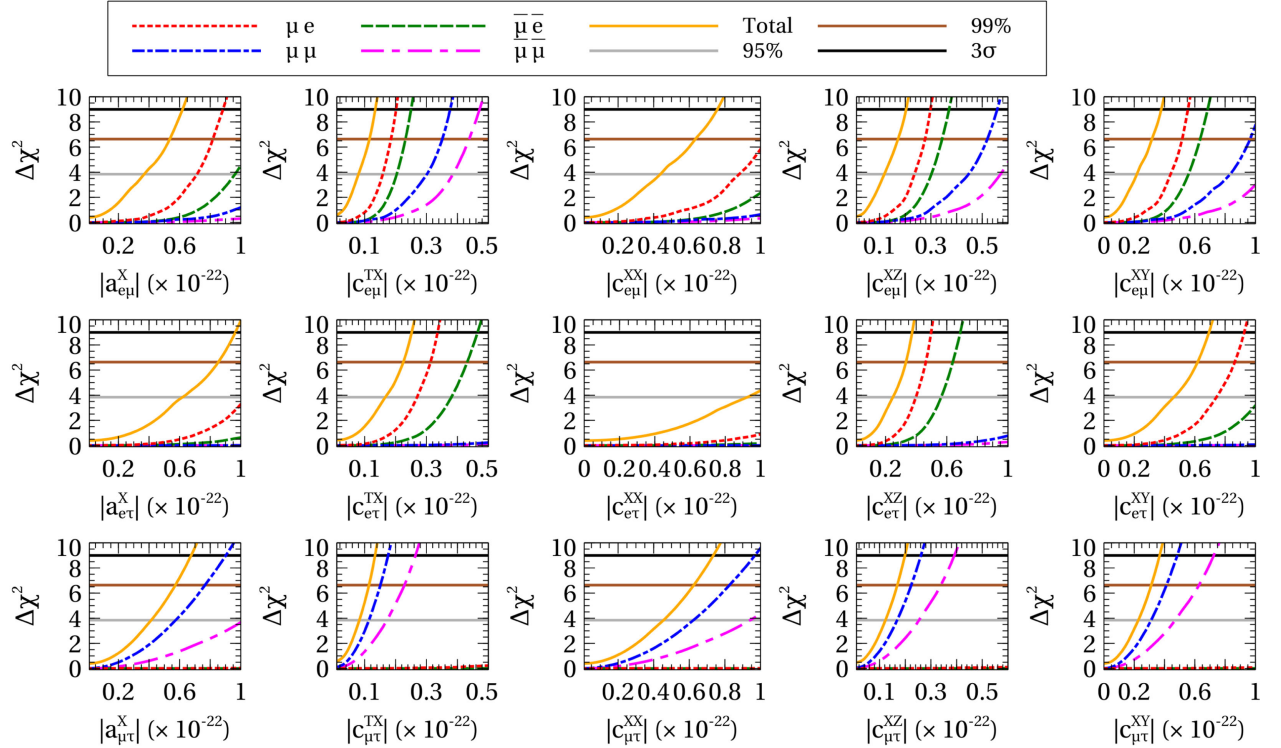

FIG. 7. Sensitivity plots of the LIV parameters for μe, $\mu\mu$, $\bar{\mu}\,\bar{e}$, $\bar{\mu}\,\overline{\mu}$, and all channels combined with 2σ and 3σ cut.

results [14,20]. This significant improvement in $a_{e\mu}^X$ ($a_{e\mu}^Y$) is attributed to the extended baseline and the combined analysis of both neutrino and antineutrino modes. In this analysis, we present the first time constraint on nondiagonal LIV parameters corresponding to the $e\tau$ coefficient, which has never been reported previously by any neutrino experiment. Only specific channels have been used in previous studies of the sidereal impact in neutrino

TABLE III. Summary of upper limits at 95 and 99.7% CL for all 27 LIV parameters under sidereal anaylsis.

Parameter	Previous limit 3σ	References	This work 95% CL	This work 99.7% CL
$\|a_{e\mu}^X\| = \|a_{e\mu}^Y\|$	2.2×10^{-20} GeV	[14,20]	3.68×10^{-23} GeV	6.18×10^{-23} GeV
$\|a_{e\tau}^X\| = \|a_{e\tau}^Y\|$	$\cdots$		6.2×10^{-23} GeV	9.64×10^{-23} GeV
$\|a_{\mu\tau}^X\| = \|a_{\mu\tau}^Y\|$	1.8×10^{-23} GeV	[16]	4.13×10^{-23} GeV	6.75×10^{-23} GeV
$\|c_{e\mu}^{TX}\| = \|c_{e\mu}^{TY}\|$	9.0×10^{-23}	[14,20]	8.0×10^{-24}	1.32×10^{-23}
$\|c_{e\tau}^{TX}\| = \|c_{e\tau}^{TY}\|$	$\cdots$		1.66×10^{-23}	2.5×10^{-23}
$\|c_{\mu\tau}^{TX}\| = \|c_{\mu\tau}^{TY}\|$	3.7×10^{-27}	[16]	8.2×10^{-24}	1.32×10^{-23}
$\|c_{e\mu}^{XX}\| = \|c_{e\mu}^{YY}\|$	4.6×10^{-21}	[14,20]	4.38×10^{-23}	7.57×10^{-23}
$\|c_{e\tau}^{XX}\| = \|c_{e\tau}^{YY}\|$	$\cdots$		9.26×10^{-23}	
$\|c_{\mu\tau}^{XX}\| = \|c_{\mu\tau}^{YY}\|$	2.5×10^{-23}	[13]	4.54×10^{-23}	7.35×10^{-23}
$\|c_{e\mu}^{XZ}\| = \|c_{e\mu}^{YZ}\|$	1.1×10^{-21}	[14,20]	1.1×10^{-23}	2.04×10^{-23}
$\|c_{e\tau}^{XZ}\| = \|c_{e\tau}^{XZ}\|$	$\cdots$		2.46×10^{-23}	3.72×10^{-23}
$\|c_{\mu\tau}^{XZ}\| = \|c_{\mu\tau}^{XZ}\|$	0.7×10^{-23}	[13]	1.21×10^{-23}	3.78×10^{-23}
$\|c_{e\mu}^{XY}\|$	2.2×10^{-21}	[14,20]	2.18×10^{-23}	3.78×10^{-23}
$\|c_{e\tau}^{XY}\|$	$\cdots$		4.62×10^{-23}	6.93×10^{-23}
$\|c_{\mu\tau}^{XY}\|$	1.2×10^{-23}	[13]	2.27×10^{-23}	3.67×10^{-23}

sectors. The NOνA experiment is explicitly designed for the appearance channel. Nevertheless, the sensitivity of $\mu\tau$ parameters is more evident in the disappearance channel. As a result, the NOνA experiment exhibits less constraint power over $\mu\tau$ parameters compared to existing bounds.

V. SUMMARY AND CONCLUSION

The presented work focuses on investigating LIV through the sidereal effect within the context of the NOνA experiment. Oscillation probabilities and events are simulated using the GLoBES software with the NOνA experimental configurations. This analysis examines the influence of the sidereal effect on various LIV parameters within the oscillation probability spectra. It is demonstrated that LIV parameters exhibit complementary characteristics in the appearance and disappearance channels. Certain parameters predominantly affect the appearance channel, while others primarily impact the disappearance channel. This pattern is also reflected in the sensitivity analysis, as sensitivity is specific to each channel.

The study suggests that the far detector of the NOνA experiment possesses the potential to enhance the existing constraints on LIV parameters. However, it is important to note that not all parameters can be thoroughly explored to achieve improved limits. Using all channels along both neutrino and antineutrino modes, far-detector data of the NOνA experiment can establish new constraints on LIV parameter values with a confidence level of 3σ under the null hypothesis. It is also noted that uncertainties of θ_{23} and δ_{CP} can reduce the sensitivity of sidereal parameters. Moreover, the sidereal parameters are highly influenced by the baseline length and neutrino energy. Future long-baseline experiments with longer baselines and higher energies, such as DUNE, T2HKK, and P2O may offer enhanced sensitivity to nonisotropic LIV parameters.
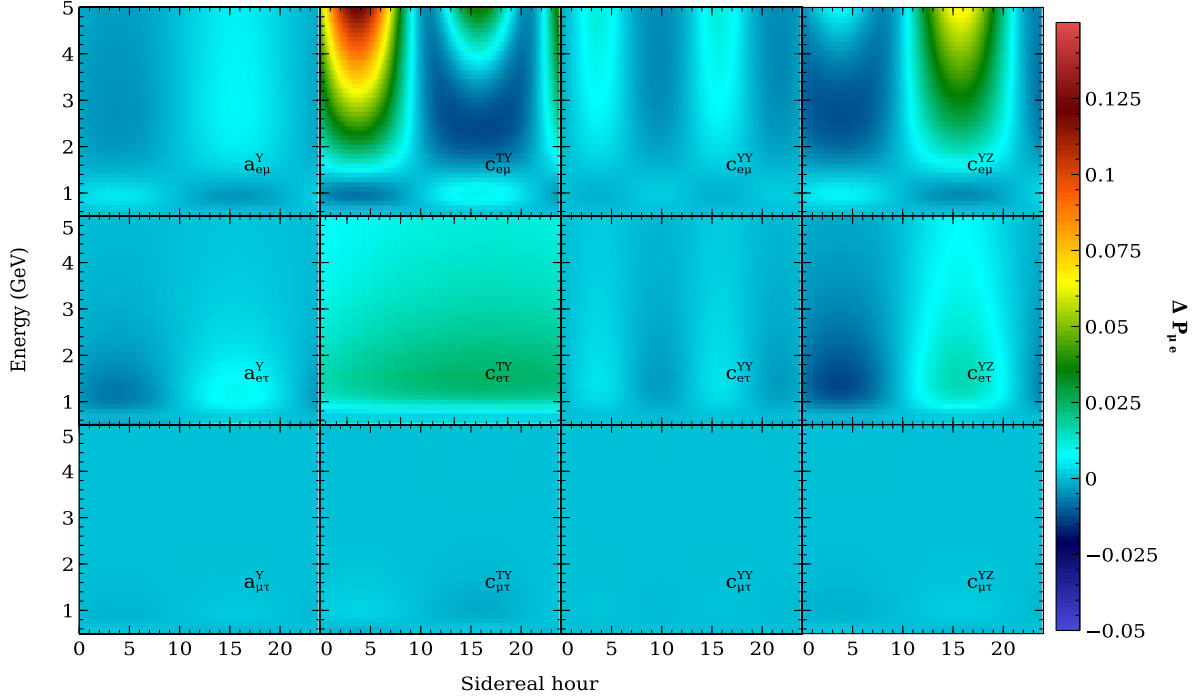
APPENDIX

FIG. 8. The probability difference distribution for the appearance channel for Y-type components ($a_{\alpha\beta}^{Y}, c_{\alpha\beta}^{TY}, c_{\alpha\beta}^{YY}, c_{\alpha\beta}^{YZ}$ with $\alpha\beta = e\mu, e\tau$, and $\mu\tau$). In each panel, one specific LIV parameter is set to 1×10^{-23}, while the others are set to 0.
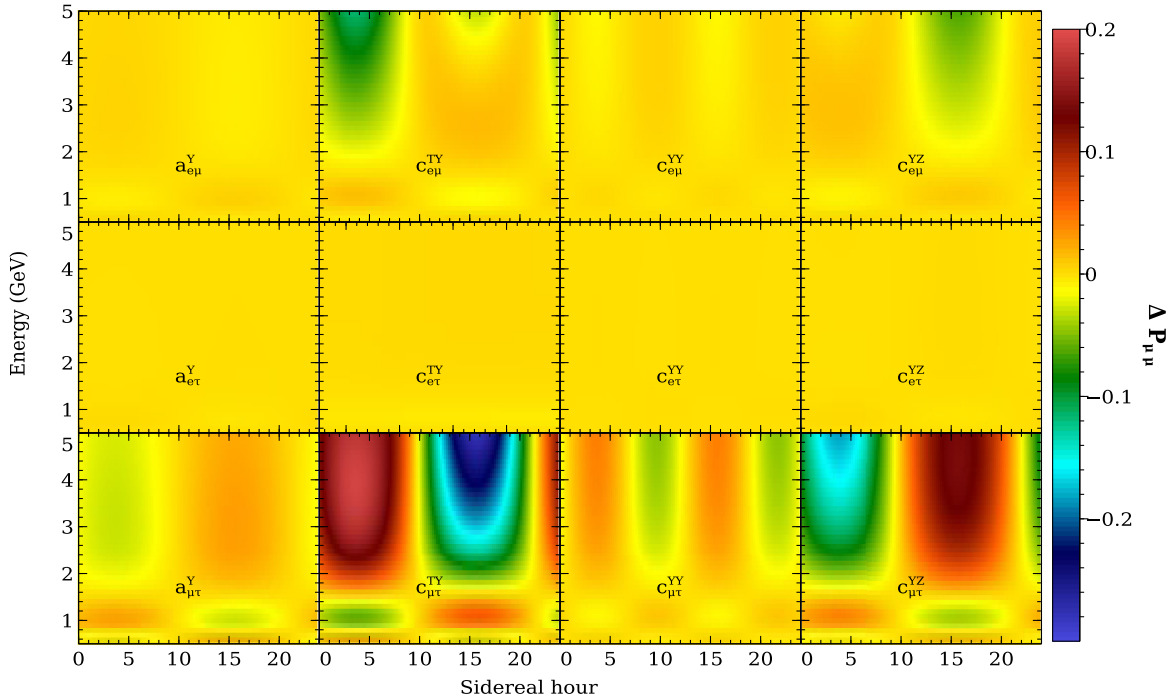

FIG. 9. The probability difference distribution for the disappearance channel for Y-type components ($a_{\alpha\beta}^{Y}, c_{\alpha\beta}^{TY}, c_{\alpha\beta}^{YY}, c_{\alpha\beta}^{YZ}$ with $\alpha\beta = e\mu$, $e\tau$, and $\mu\tau$). In each panel, one specific LIV parameter is set to 1×10^{-23}, while the others are set to 0.

[1] V. A. Kostelecky and S. Samuel, Spontaneous breaking of Lorentz symmetry in string theory, Phys. Rev. D **39,** 683 (1989).

[2] V. A. Kostelecky and R. Potting, *CPT* and strings, Nucl. Phys. **B359,** 545 (1991).

[3] R. Gambini and J. Pullin, Nonstandard optics from quantum space-time, Phys. Rev. D **59,** 124021 (1999).

[4] C. P. Burgess, J. M. Cline, E. Filotas, J. Matias, and G. D. Moore, Loop-generated bounds on changes to the graviton dispersion relation, J. High Energy Phys. 03 (2002) 043.

[5] S. Sahoo, A. Kumar, and S. K. Agarwalla, Probing Lorentz invariance violation with atmospheric neutrinos at INO-ICAL, J. High Energy Phys. 03 (2022) 050.

[6] D. Colladay and V. A. Kostelecky, Lorentz violating extension of the standard model, Phys. Rev. D **58,** 116002 (1998).

[7] R. Bluhm, Overview of the SME: Implications and phenomenology of Lorentz violation, Lect. Notes Phys. **702,** 191 (2006).

[8] V. A. Kostelecký and N. Russell, Data tables for Lorentz and *CPT* violation, Rev. Mod. Phys. **83,** 11 (2011).

[9] Y. Fukuda *et al.* (Super-Kamiokande Collaboration), Measurements of the solar neutrino flux from Super-Kamiokande's first 300 days, Phys. Rev. Lett. **81,** 1158 (1998); **81,** 4279 (1998).

[10] K. Eguchi *et al.* (KamLAND Collaboration), First results from KamLAND: Evidence for reactor anti-neutrino disappearance, Phys. Rev. Lett. **90,** 021802 (2003).

[11] M. H. Ahn *et al.* (K2K Collaboration), Measurement of neutrino oscillation by the K2K experiment, Phys. Rev. D **74,** 072003 (2006).

[12] L. B. Auerbach *et al.* (LSND Collaboration), Tests of Lorentz violation in $\bar{\nu}_\mu \rightarrow \bar{\nu}_e$ oscillations, Phys. Rev. D **72,** 076004 (2005).

[13] P. Adamson *et al.* (MINOS Collaboration), A search for Lorentz invariance and *CPT* violation with the MINOS far detector, Phys. Rev. Lett. **105,** 151601 (2010).

[14] P. Adamson *et al.* (MINOS Collaboration), Search for Lorentz invariance and *CPT* violation with muon antineutrinos in the MINOS near detector, Phys. Rev. D **85,** 031101 (2012).

[15] A. A. Aguilar-Arevalo *et al.* (MiniBooNE Collaboration), Test of Lorentz and *CPT* violation with short baseline neutrino oscillation excesses, Phys. Lett. B **718,** 1303 (2013).

[16] R. Abbasi *et al.* (IceCube Collaboration), Search for a Lorentz-violating sidereal signal with atmospheric neutrinos in IceCube, Phys. Rev. D **82,** 112003 (2010).

[17] Y. Abe *et al.* (Double Chooz Collaboration), First test of Lorentz violation with a reactor-based antineutrino experiment, Phys. Rev. D **86,** 112009 (2012).

[18] K. Abe *et al.* (T2K Collaboration), Search for Lorentz and *CPT* violation using sidereal time dependence of neutrino flavor transitions over a short baseline, Phys. Rev. D **95,** 111101 (2017).

[19] D. Adey *et al.* (Daya Bay Collaboration), Search for a time-varying electron antineutrino signal at Daya Bay, Phys. Rev. D **98,** 092013 (2018).

[20] P. Adamson *et al.* (MINOS Collaboration), Testing Lorentz invariance and *CPT* conservation with NuMI neutrinos in the MINOS near detector, Phys. Rev. Lett. **101,** 151601 (2008).

[21] K. Abe *et al.* (Super-Kamiokande Collaboration), Test of Lorentz invariance with atmospheric neutrinos, Phys. Rev. D **91,** 052003 (2015).

[22] M. A. Acero *et al.* (NOνA Collaboration), First measurement of neutrino oscillation parameters using neutrinos and antineutrinos by NOνA, Phys. Rev. Lett. **123,** 151803 (2019).

[23] J. S. Diaz, V. A. Kostelecky, and M. Mewes, Perturbative Lorentz and *CPT* violation for neutrino and antineutrino oscillations, Phys. Rev. D **80,** 076007 (2009).

[24] J. Kopp, M. Lindner, T. Ota, and J. Sato, Non-standard neutrino interactions in reactor and superbeam experiments, Phys. Rev. D **77,** 013007 (2008).

[25] V. A. Kostelecky and M. Mewes, Lorentz and *CPT* violation in the neutrino sector, Phys. Rev. D **70,** 031902 (2004).

[26] V. A. Kostelecky and M. Mewes, Lorentz violation and short-baseline neutrino experiments, Phys. Rev. D **70,** 076002 (2004).

[27] J. Liao, D. Marfatia, and K. Whisnant, Degeneracies in long-baseline neutrino experiments from nonstandard interactions, Phys. Rev. D **93,** 093016 (2016).

[28] M. Esteves Chaves, D. Rossi Gratieri, and O. L. G. Peres, Improvements on perturbative oscillation formulas including non-standard neutrino interactions, J. Phys. G **48,** 015001 (2020).

[29] U. K. Dey, N. Nath, and S. Sadhukhan, Non-standard neutrino interactions in a modified ν2HDM, Phys. Rev. D **98,** 055004 (2018).

[30] O. Yasuda, On the exact formula for neutrino oscillation probability by Kimura, Takamura and Yokomakura, arXiv:0704.1531.

[31] M. Masud, A. Chatterjee, and P. Mehta, Probing *CP* violation signal at DUNE in presence of non-standard neutrino interactions, J. Phys. G **43,** 095005 (2016).

[32] M. Masud and P. Mehta, Nonstandard interactions spoiling the *CP* violation sensitivity at DUNE and other long baseline experiments, Phys. Rev. D **94,** 013014 (2016).

[33] M. Masud and P. Mehta, Nonstandard interactions and resolving the ordering of neutrino masses at DUNE and other long baseline experiments, Phys. Rev. D **94,** 053007 (2016).

[34] R. Majhi, S. Chembra, and R. Mohanta, Exploring the effect of Lorentz invariance violation with the currently running long-baseline experiments, Eur. Phys. J. C **80,** 364 (2020).

[35] D. S. Ayres *et al.* (NOνA Collaboration), The NOνA technical design report, Report No. FERMILAB-DESIGN-2007-01, 2007, 10.2172/935497.

[36] P. Huber, M. Lindner, and W. Winter, Simulation of long-baseline neutrino oscillation experiments with GLoBES (General Long Baseline Experiment Simulator), Comput. Phys. Commun. **167,** 195 (2005).

[37] P. Huber, J. Kopp, M. Lindner, M. Rolinec, and W. Winter, New features in the simulation of neutrino oscillation experiments with GLoBES3.0: General long baseline experiment simulator, Comput. Phys. Commun. **177,** 432 (2007).

[38] P. B. Denton and J. Gehrlein, Here comes the sun: Solar parameters in long-baseline accelerator neutrino oscillations, J. High Energy Phys. 06 (2023) 090.

[39] I. Esteban, M. C. Gonzalez-Garcia, M. Maltoni, T. Schwetz, and A. Zhou, The fate of hints: Updated global analysis of three-flavor neutrino oscillations, J. High Energy Phys. 09 (2020) 178.

[40] S. Baker and R. D. Cousins, Clarification of the use of CHI-square and likelihood functions in fits to histograms, Nucl. Instrum. Methods Phys. Res. **221,** 437 (1984).